Electrochimica Acta 182 (2015) 342–350

Contents lists available at ScienceDirect

Electrochimica Acta

journal homepage: www.elsevier.com/locate/electacta

Seebeck coefficients of cells with molten carbonates relevant for the metallurgical industry

X. Kang[b], M.T. Børset[a], O.S. Burheim[c], G.M. Haarberg[d], Q. Xu[e], S. Kjelstrup[a,*]

[a] Department of Chemistry, Norwegian University of Science and Technology, NO-7491 Trondheim, Norway
[b] School of Materials Science and Metallurgy, Northeastern University, Shenyang, Liaoning, 110819, China
[c] Faculty of Technology, Sør-Trøndelag University College, Trondheim, Norway
[d] Department of Materials Technology and Engineering, Norwegian University of Science and Technology, NO-7491 Trondheim, Norway
[e] School of materials Science and Engineering, Shanghai University, Shanghai, 200072, China

ARTICLE INFO

Article history:
Received 3 June 2015
Received in revised form 2 August 2015
Accepted 10 September 2015
Available online 15 September 2015

Keywords:
Seebeck coefficient
Transported entropy
Thermoelectric
Molten carbonates
Thermocell

ABSTRACT

We report Seebeck coefficients of electrochemical cells with molten carbonate mixtures as electrolytes and carbon dioxide|oxygen electrodes. The system is relevant for use of waste heat and off-gases with concentration of carbon dioxide different from air, as for example in the metallurgical industry. The coefficient is $-1.25\,mV\,K^{-1}$ for a nearly equimolar mixture of lithium and sodium carbonate with dispersed magnesium oxide at 750 °C, one bar total pressure and a pressure ratio of carbon dioxide to oxygen of 2:1. The value is slightly lower when sodium is replaced by potassium. The theoretical expression of the Seebeck coefficient was established using the theory of non-equilibrium thermodynamics. We used this expression to predict an increase to $-1.4\,mV\,K^{-1}$ when lowering the gas partial pressures to 0.015 and 0.2 bar, respectively, for carbon dioxide and oxygen, a gas composition that can represent that of the off-gases from a silicon furnace which we are concerned with. The absolute value of the Seebeck coefficient increases by $0.2\,mV\,K^{-1}$ when the cell average temperature increases from 550 to 850 °C. The presence of a second component in the electrolyte increases the coefficient significantly above the values obtained with one component, compatible with a lowering of the transported entropy of the carbonate ion. A concentration cell, using the off-gas from the silicon furnace as anode gas and air as cathode gas, will add 0.14 V at 550°C to the absolute value of the potential. The series construction has the potential to offer a power density at matched load conditions in the order of $0.5\,kW\,m^{-2}$.

© 2015 The Authors. Published by Elsevier Ltd. This is an open access article under the CC BY-NC-ND license (http://creativecommons.org/licenses/by-nc-nd/4.0/).

1. Introduction

We are pursuing an investigation of electrochemical cells with cheap ionic conductors and gas electrodes, for the purpose of thermoelectric power production from industrial waste heat [1]. The Seebeck effect, the electric potential produced by a temperature difference between the electrodes, originates from the reversible heat changes connected with the electrode reactions and with the charge transport in the electrolyte, see *e.g.*, Agar [2]. So far, research on thermoelectricity has concentrated on semiconducting materials [3,4], but prospects of larger Seebeck coefficients, combined with potentially cheaper, more benign and environmentally friendly materials, is now motivating research on ion-conducting materials [5,6].

We are targeting waste heat recovery from the metallurgical industry, in particular from the production of silicon [7]. Thermal energy is here available from 1600 °C down to room temperature [8–10]. In addition, these industries are often emitting carbon dioxide at a different composition than the surrounding air, thus representing an additional power source [11]. Our candidate system is a molten alkali carbonate cell with carbon dioxide|oxygen electrodes. It has earlier been studied in connection with fuel cells and has a large Seebeck coefficient. Values around $-1.20\,mV\,K^{-1}$ was measured for molten binary and ternary mixtures of alkali carbonates in the range 530 to 880 °C [12]. An electrochemical cell operating in this temperature window, can therefore utilize a large temperature difference, as well as the potential energy present in the off-gas.

We have recently examined the cell with pure lithium carbonate as the electrolyte [1]. It was shown, that the electrode reaction (the conversion of carbon dioxide to carbonate ion), contributed

* Corresponding author.
E-mail addresses: kx81@163.com (X. Kang), marit.takla.borset@ntnu.no (M.T. Børset), odnesb@hist.no (O.S. Burheim), geir.martin.haarberg@ntnu.no (G.M. Haarberg), qianxu@shu.edu.cn (Q. Xu), signe.kjelstrup@ntnu.no (S. Kjelstrup).

http://dx.doi.org/10.1016/j.electacta.2015.09.059
0013-4686/© 2015 The Authors. Published by Elsevier Ltd. This is an open access article under the CC BY-NC-ND license (http://creativecommons.org/licenses/by-nc-nd/4.0/).

Table 1
The composition of the electrolytes, as given by molar fractions x_j, and the corresponding melting point temperature (T_m)[22].

Cell	Electrolyte	$x_{Li_2CO_3}$	$x_{Na_2CO_3}$	$x_{K_2CO_3}$	T_m
LNC-MgO	$(Li_{x_1}Na_{x_2})_2CO_3$	0.53	0.47	-	500 °C
LKC-MgO	$(Li_{x_1}K_{x_2})_2CO_3$	0.62	-	0.38	488 °C

largely to the Seebeck coefficient. Also important was the addition of an inorganic powder to the melt, enhancing the Seebeck coefficient significantly, and lowering simultaneously the transported entropy of the carbonate ion. A possible explanation of this, was the lowering of the entropy of the salt in the dispersion of the solid [13]. Here, we expand on these studies [1] by using binary mixtures of molten alkali carbonates. Two-component electrolytes have not been investigated for thermoelectric energy conversion since the early investigations of Jacobsen and Broers [12].

In terms of non-equilibrium thermodynamic theory, the Seebeck effect originate from the coupling of heat and charge transfer. This theory gives a framework from which experiments can be defined [14]. It must be used to derive the relation between the Seebeck coefficient and the Peltier heat, as well as other relations between transport properties. For instance, one can find from the invariance of the entropy production that the thermodynamic entropy of one salt is equal to the sum of transported entropies of the ions in a one-component electrolyte [2,15,16,1]. Electrochemical systems have been evaluated with non-equilibrium theory in the past, see *e.g.*, Agar [2] and Førland et. al. [16], but the theory is now able to deal with electrode surfaces more directly, see [17]. We shall use the method as developed for heterogeneous systems in Section 2.2 [17]. Readers not interested in theoretical details can skip the derivations in 2.2 and go directly from Section 2.1 (System description) to the equations used to interpret the experimental results, see Sections 2.3 and 2.4.

2. Theory

2.1. System description

Consider a cell with gas electrodes, reversible to the carbonate ion, held at different temperatures:

$$\mathrm{Au}\left(T^{s,a}\right)|\mathrm{CO_2(g)},\mathrm{O_2(g)}|(\mathrm{Li,M})_2\mathrm{CO_3(l)},\mathrm{MgO(s)}|\mathrm{CO_2(g)},\mathrm{O_2(g)}|\mathrm{Au}\left(T^{s,c}\right) \quad \text{(LMC-MgO)}$$

The label LMC-MgO refers to a dispersion of a binary alkali carbonate and magnesium oxide, where LMC designate the binary alkali carbonate mixture. The L refer to lithium ion and the M to either sodium- or potassium ion and C to carbonate ion. The mixture is an eutectic one, providing a relatively low melting point (compositions are given in Table 1). The molten electrolyte is mixed with magnesium oxide powder (45*wt*%:55*wt*% MgO) and the result is a dispersion of MgO particles in the carbonate electrolyte. The cell has two carbon dioxide|oxygen electrodes, kept at different temperatures $T^{s,a}$ and $T^{s,c}$, immersed in the electrolyte. The electrode gas is in contact with a metal conductor, here of gold, and we use the same gas composition at both electrodes. The electrochemical reaction at the left-hand side electrode is [12]:

$$\frac{1}{2}CO_3^{2-}(l) \rightarrow \frac{1}{2}CO_2(g) + \frac{1}{4}O_2(g) + e^- \quad (1)$$

The reverse reaction takes place at the right-hand side. We divide the cell into five subsystems; the left and right electronic conductors (a and c), the two electrode surfaces (s,a and s,c) and the electrolyte (e). The notation is illustrated in Fig. 1a. Fig. 1b shows a cross section of the cell.

The Seebeck coefficient is the measured potential difference divided by the temperature difference between the electrodes in the limits $j \rightarrow 0$ and $T^{s,c} - T^{s,a} = \Delta T \rightarrow 0$. We measure the emf of LMC-MgO between two Cu wires attached to the Au wires at room temperature ($T^{a,o} = T^{c,o} = T^0$, see Fig. 1a). The cell emf is the sum of the potential difference across each subsystem:

$$\Delta\phi = \phi_c - \phi_a = \Delta_a\phi + \Delta_{a,e}\phi + \Delta_e\phi + \Delta_{e,c}\phi + \Delta_c\phi \quad (2)$$

The Seebeck coefficient and its various contributions is accordingly:

$$\alpha_S \equiv \left(\frac{\Delta\phi}{\Delta T}\right)_{j\rightarrow 0,\Delta T\rightarrow 0} = \frac{\Delta_a\phi + \Delta_c\phi}{\Delta T} + \frac{\Delta_{a,e}\phi + \Delta_{e,c}\phi}{\Delta T} + \frac{\Delta_e\phi}{\Delta T} \quad (3)$$

where we assumed constant temperature across each surface, *i.e.* $T^{a,e} = T^{s,a} = T^{e,a}$ and $T^{e,c} = T^{s,c} = T^{c,e}$, *c.f.* Fig. 1a. We establish below the expressions for α_S. The results are given in Sections 2.4 and 2.3.

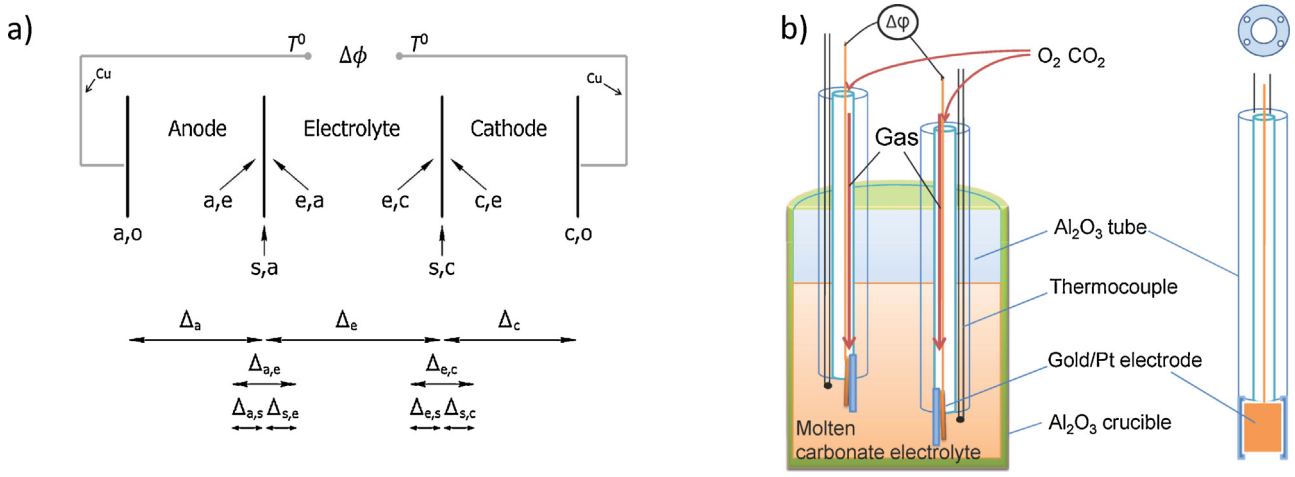

Fig. 1. A schematic picture of the cell (a) and a cross section of the experimental cell with electrodes (b). In a) we show the five subsystems of the cell and the notation used for transport properties. The first superscript refers to the phase in question, and the second to the neighboring phase. A Δ with one subscript, i, denotes the difference across phase i. A Δ with two subscripts, i, k, denotes the value in phase k minus the value in phase i. In b) we show a cross section of the cell used in the experiments. The electrodes consist of a gold wire which is point-welded to a gold plate (the electrode surface). We used a five bore alumina tube as insulation for thermocouples and electrodes. A cross section of this tube is shown above the electrode in the figure.

2.2. Application of non-equilibrium thermodynamics

The general procedure to find the thermoelectric potential from this theory is to determine the subsystem entropy production and the flux equations that follow from this. The equations for the metallic conductors (a and c), are well known, so we repeat only the final equation. The electrode surfaces and the electrolyte have more complicated expressions, not given before. We will hence treat these subsystems in more detail, starting with the entropy production.

2.2.1. The conductors connecting the cell

By integrating the expression for the electric potential from the temperature of the surroundings, T^0, to the electrode temperature $T^{s,a}$ on the left hand-side, and from the electrode temperature on the right-hand side, $T^{s,c}$, to T^0, we find the well-known contributions from the conductors to the cell potential, see *e.g.* [17]:

$$\frac{\Delta_a\phi + \Delta_c\phi}{\Delta T} = -\frac{1}{F}S_e^* \tag{4}$$

Here S_e^* is the transported entropy of the electron, this was assumed constant in the temperature interval, and F is Faraday's constant.

2.2.2. The electrode surfaces

The excess entropy production in the anode surface (s,a) has two terms related to heat transfer across the surface, four terms related to possible lack of equilibrium for adsorption of gases or salts, one term due to the electric power and one to the electrochemical reaction [17]:

$$\begin{aligned}\sigma^{s,a} &= J_q'^{a,e}\Delta_{a,s}\left(\frac{1}{T}\right) + J_q'^{e,a}\Delta_{s,e}\left(\frac{1}{T}\right)\\ &\quad -\frac{1}{T^{s,a}}\left(J_{O_2}^{e,a}\Delta_{s,e}\mu_{O_2,T} + J_{CO_2}^{e,a}\Delta_{s,e}\mu_{CO_2,T}\right)\\ &\quad -\frac{1}{T^{s,a}}\left(J_1^{e,a}\Delta_{s,e}\mu_{1,T} + J_2^{e,a}\Delta_{s,e}\mu_{2,T}\right)\\ &\quad -\frac{1}{T^{s,a}}\left(j\Delta_{a,e}\phi + r^s\Delta_n G^{s,a}\right)\end{aligned} \tag{5}$$

where J_q' is the measurable heat flux, J_j is the flux of component j, j is the current density and subscripts 1 and 2 refer to Li^+- and M^+-carbonate, respectively, $\Delta_n G^{s,a}$ is the reaction Gibbs energy expressed in terms of neutral components. See [17] and Fig. 1a for further explanation of the notation. When the electrodes are thermostatted, we have constant temperature across the surface (i.e. $T^{a,e} = T^{s,a} = T^{e,a}$) and with chemical equilibrium for adsorbed components (i.e. $\mu_{j,T}^{s,a} = \mu_{j,T}^{e,a}$), only the last two terms remain. For reversible conditions $\sigma^{s,a} = 0$, and the reaction rate is $r^s = j/F$. The electrode potential jump is simply:

$$\Delta_{a,e}\phi = -\Delta_n G^{s,a}/F \tag{6}$$

There are only two contributions to $\Delta_n G^{s,a}$; from the production of CO_2 and O_2 at the electrode see Eq. (1). This gives:

$$\Delta_{a,e}\phi = -\frac{1}{F}\left(\frac{1}{2}\mu_{CO_2}^{s,a}\left(T^{s,a}\right) + \frac{1}{4}\mu_{O_2}^{s,a}\left(T^{s,a}\right)\right) \tag{7}$$

The same analysis applies to the right-hand surface. The total contribution from the electrodes to the cell potential is then:

$$\frac{\Delta_{a,e}\phi + \Delta_{e,c}\phi}{\Delta T} = -\frac{1}{F}\left(\frac{1}{2}S_{CO_2} + \frac{1}{4}S_{O_2}\right) \tag{8}$$

We used the relation $\left(\partial\mu_j/\partial T\right)_p = -S_j$ to obtain the last equality. Again we have taken the entropy to be constant in the temperature interval, and shall evaluate S_j at the average of the electrode temperatures.

2.2.3. Contribution from the electrolyte

The entropy production is the sum of the products of the conjugate fluxes and forces in the system. The electrolyte has three (neutral) components: the two molten alkali carbonates and the magnesium oxide powder in the solid state. The oxide has a constant chemical potential since it is present in the solid state, and does not contribute to the entropy production. The carbon dioxide and oxygen gas can dissolve in the electrolyte, but since the partial pressures of oxygen and carbon dioxide are constant throughout the system, it does not contribute to the entropy production. The chemical potential gradients of the two remaining components are related by Gibbs-Duhem's equation, $d\mu_{1,T} = -x_2 d\mu_{2,T}/x_1$. There are then three independent driving forces in the entropy production: one thermal driving force($\frac{d}{dz}\frac{1}{T}$), one component driving force ($-\frac{1}{T}\frac{d\mu_{2,T}}{dz}$) plus the force containing the gradient in electric potential ($-\frac{1}{T}\frac{d\phi}{dz}$):

$$\begin{aligned}\sigma^e &= J_q'^e\left(\frac{d}{dz}\frac{1}{T}\right) + J_2\left(-\frac{1}{T}\frac{d\mu_{2,T}}{dz}\right) + J_1\left(\frac{x_2}{x_1}\frac{1}{T}\frac{d\mu_{2,T}}{dz}\right) + j\left(-\frac{1}{T}\frac{d\phi}{dz}\right)\\ &= J_q'^e\left(\frac{d}{dz}\frac{1}{T}\right) + \left(\frac{J_2}{x_2} - \frac{J_1}{x_1}\right)\left(-\frac{x_2}{T}\frac{d\mu_{2,T}}{dz}\right) + j\left(-\frac{1}{T}\frac{d\phi}{dz}\right)\\ &= J_q'^e\left(\frac{d}{dz}\frac{1}{T}\right) + J_{21}\left(-\frac{x_2}{T}\frac{d\mu_{2,T}}{dz}\right) + j\left(-\frac{1}{T}\frac{d\phi}{dz}\right)\end{aligned} \tag{9}$$

The mole fractions are $x_2 = x_{M_2CO_3} = n_{M_2CO_3}/\left(n_{Li_2CO_3} + n_{M_2CO_3}\right)$ and $x_1 = 1 - x_2$. The flux J_{21} is the flux of M_2CO_3 relative to the flux of Li_2CO_3, each weighted by the respective mole fraction, so the second term on the right hand side describes the energy dissipated by interdiffusion of the components.

From Eq. (9), we write the flux equations for transport of heat, mass and charge in the electrolyte as:

$$J_q'^e = L_{qq}^e\left(-\frac{1}{T^2}\frac{dT}{dz}\right) + L_{q\mu}^e\left(-\frac{x_2}{T}\frac{d\mu_{2,T}}{dz}\right) + L_{q\phi}^e\left(-\frac{1}{T}\frac{d\phi}{dz}\right) \tag{10}$$

$$J_{21} = L_{\mu q}^e\left(-\frac{1}{T^2}\frac{dT}{dz}\right) + L_{\mu\mu}^e\left(-\frac{x_2}{T}\frac{d\mu_{2,T}}{dz}\right) + L_{\mu\phi}^e\left(-\frac{1}{T}\frac{d\phi}{dz}\right) \tag{11}$$

$$j = L_{\phi q}^e\left(-\frac{1}{T^2}\frac{dT}{dz}\right) + L_{\phi\mu}^e\left(-\frac{x_2}{T}\frac{d\mu_{2,T}}{dz}\right) + L_{\phi\phi}^e\left(-\frac{1}{T}\frac{d\phi}{dz}\right) \tag{12}$$

The coefficients (L's) depend on the local state variables (e.g., temperature and pressure), but are *independent* of the forces. All forces contribute to each flux in the electrolyte. The coefficients describe the contribution from the force to the flux and they are related through the Onsager reciprocal relations as $L_{ij} = L_{ji}$.

From Eq. (12) we express the gradient in the electric potential, at any time, as:

$$\frac{d\phi}{dz} = -\frac{\pi^e}{TF}\frac{dT}{dz} - \frac{t_{21}}{F}x_2\frac{d\mu_{2,T}}{dz} - r^e j \tag{13}$$

where the gradient terms may vary with time due to thermal diffusion. In Eq. (13), π^e is the Peltier coefficient of the electrolyte, t_{21} is the transference coefficient connected with the relative flux J_{21} and r^e is the electrical resistivity of the electrolyte. The Peltier coefficient is defined as the heat transported *reversibly* with the current:

$$\begin{aligned}\pi^e &\equiv \left(\frac{J_q'^e}{j/F}\right)_{dT=0,d\mu_T=0} = F\frac{L_{q\phi}^e}{L_{\phi\phi}^e}\\ &= \left(\frac{T\left(J_S^e - (J_2S_2 + J_1S_1)\right)}{j/F}\right)_{dT=0,d\mu_T=0}\end{aligned} \tag{14}$$

where we expressed the measurable heat flux in terms of the entropy flux J_S^e and the entropy flux caused by the flux of the components to obtain the last equality. The transference coefficient is the number of moles transferred per mole electric charge:

$$t_{21} \equiv \left(\frac{J_{21}}{j/F}\right)_{dT=0,d\mu_T=0} = \left(\frac{t_2}{x_2} - \frac{t_1}{x_1}\right) = F\frac{L^e_{\mu\phi}}{L^e_{\phi\phi}} \tag{15}$$

where the coefficients t_2 and t_1 are, respectively, the transference coefficients of M_2CO_3 and Li_2CO_3. In a mixture of uniform composition (i.e. at initial time) $d\mu_{2,T} = d\mu_{1,T} = 0$. We integrate Eq. (13) across the electrolyte, from $T^{s,a}$ to $T^{s,c}$ at $j \approx 0$, and express the contribution from the electrolyte to the Seebeck coefficient at initial time (indicated by $t = 0$) as:

$$\left(\frac{\Delta\phi_e}{\Delta T}\right)_{t=0} = -\frac{\pi^e}{TF} \tag{16}$$

As stated in the Introduction, we obtain a relation between the Seebeck coefficient and the Peltier heat using an Onsager relation. We took the ratio π^e/T to be constant across the temperature interval. From Eq. (14), we can interpret this ratio as an entropy related to transport of charge in the electrolyte.

A stationary state will develop, with a balance between the chemical and the thermal driving force. This is called Soret equilibrium. The stationary state condition gives $J_2 = J_1 = J_{21} = 0$, and the emf measurement has $j \approx 0$. Then, from Eq. (11), we find that the balance condition reads:

$$-x_2\frac{d\mu_{2,T}}{dz} = \frac{q^*}{T}\frac{dT}{dz} \tag{17}$$

where the heat of transfer for the *interdiffusion* of M_2CO_3 and Li_2CO_3, q^*, is defined as:

$$q^* \equiv \left(\frac{J_q^e}{J_{21}}\right)_{dT=0,j=0} = \frac{\left(L^e_{q\mu} - \frac{L^e_{q\phi}L^e_{\phi\mu}}{L^e_{\phi\phi}}\right)}{\left(L^e_{\mu\mu} - \frac{L^e_{\mu\phi}L^e_{\phi\mu}}{L^e_{\phi\phi}}\right)} \tag{18}$$

We introduce Eqs. (17) and (15) into Eq. (13) and integrate across the electrolyte for $j \approx 0$. The contribution from the electrolyte to the Seebeck coefficient at stationary state (Soret equilibrium, indicated by ∞) is:

$$\left(\frac{\Delta\phi_e}{\Delta T}\right)_\infty = -\frac{1}{F}\left(\frac{\pi^e}{T} - \left(\frac{t_2}{x_2} - \frac{t_1}{x_1}\right)\frac{q^*}{T}\right) \tag{19}$$

Here we took both ratios π^e/T and q^*/T to be constant across the temperature interval. The ratio q^*/T, may be interpreted in terms of enthalpy changes across the layer [17].

We need a more explicit expression for the Peltier coefficient, π^e. This can be found from the entropy balance of a volume element in the electrolyte at reversible conditions (isothermal and uniform concentrations). We use the definitions of the Peltier and the transference coefficients, Eqs. (14) and (15), to express the Peltier coefficient in terms of transported entropies of the carbonate ion and the cations L^+ and M^+. This will give a relation between the transported entropies of the ions, the thermodynamic entropy of the salt and the heat of transfer in the binary mixture.

The oxide MgO is only slightly soluble in the electrolyte [18], meaning that it is fair to neglect Mg^{2+} and O^{2-} as charge transporters. All transport of charge is then taking place by three ions and the sum of transport numbers equals unity, $t_{CO_3^{2-}} + t_{M^+} + t_{Li^+} = 1$. The transference coefficients of components 1 and 2 (see Eq. (15)) require a definition of the frame of reference for the mass fluxes, and we choose the wall frame of reference [19]. The transference coefficient can be interpreted by the transport numbers of the cations, see Fig. 2, as follows:

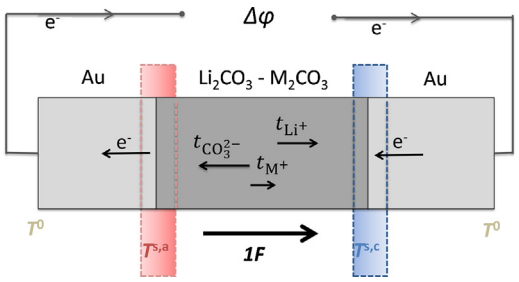

Fig. 2. A schematic drawing of the cell, illustrating transport of ions in the electrolyte.

$$t_1 = t_{Li_2CO_3} = \frac{1}{2}t_{Li^+} \quad t_2 = t_{M_2CO_3} = \frac{1}{2}t_{M^+} \tag{20}$$

We introduce these into Eq. (14), and find π^e of the electrolyte from the balance of reversible effects:

$$\frac{\pi^e}{T} = -\frac{1}{2}S^*_{CO_3^{2-}} + t_{M^+}(S^*_{M^+} + \frac{1}{2}S^*_{CO_3^{2-}} - \frac{1}{2}S_2) + t_{Li^+}(S^*_{Li^+} + \frac{1}{2}S^*_{CO_3^{2-}} - \frac{1}{2}S_1) \tag{21}$$

With Eqs. (19) and (21), we find the contribution from the electrolyte to the Seebeck coefficient at $J_{21} = 0$ as:

$$\left(\frac{\Delta\phi}{\Delta T}\right)_\infty = -\frac{1}{F}\left(-\frac{1}{2}S^*_{CO_3^{2-}} + t_{M^+}(S^*_{M^+} + \frac{1}{2}S^*_{CO_3^{2-}} - \frac{1}{2}S_2 - \frac{1}{2x_2}\frac{q^*}{T}) + t_{Li^+}(S^*_{Li^+} + \frac{1}{2}S^*_{CO_3^{2-}} - \frac{1}{2}S_1 + \frac{1}{2x_1}\frac{q^*}{T})\right) \tag{22}$$

Because the electric potential is independent of the frame of reference used for the mass fluxes, the sums in the parentheses must be zero (cannot depend on the transport numbers). We obtain:

$$t_{M^+}(S^*_{M^+} + \frac{1}{2}S^*_{CO_3^{2-}} - \frac{1}{2}S_2) + t_{Li^+}(S^*_{Li^+} + \frac{1}{2}S^*_{CO_3^{2-}} - \frac{1}{2}S_1) = \left(\frac{t_2}{x_2} - \frac{t_1}{x_1}\right)\frac{q^*}{T} \tag{23}$$

We introduce this into Eq. (21) and find the contribution from the electrolyte at uniform composition:

$$\left(\frac{\Delta\phi_e}{\Delta T}\right)_{t=0} = -\frac{1}{F}\left(-\frac{1}{2}S^*_{CO_3^{2-}} + \left(\frac{t_2}{x_2} - \frac{t_1}{x_1}\right)\frac{q^*}{T}\right) \tag{24}$$

At Soret equilibrium, the expression for the one-component electrolyte applies, *c.f.* [1]:

$$\left(\frac{\Delta\phi_e}{\Delta T}\right)_\infty = -\frac{1}{F}\left(-\frac{1}{2}S^*_{CO_3^{2-}}\right) \tag{25}$$

2.3. The Seebeck coefficient of cell LMC-MgO at initial conditions

According to the procedure above, the Seebeck coefficient at uniform melt composition (short times) is:

$$\alpha_{S,0} = -\frac{1}{F}\left[\frac{1}{2}S_{CO_2} + \frac{1}{4}S_{O_2} + S^*_e - \frac{1}{2}S^*_{CO_3^{2-}} + \left(\frac{t_2}{x_2} - \frac{t_1}{x_1}\right)\frac{q^*}{T}\right] \tag{26}$$

Equation (23) gives a relation between the transported entropies of the ions:

$$2(S^*_{M^+} - S^*_{Li^+}) = S_2 - S_1 + (\frac{t_{M^+}}{x_2} - \frac{t_{Li^+}}{x_1})\frac{q^*}{T} \tag{27}$$

This gives

$$\begin{aligned} S^*_{CO_3^{2-}} + 2S^*_{M^+} &= S_2 + \frac{t_2}{x_2}\frac{q^*}{T} \\ S^*_{CO_3^{2-}} + 2S^*_{Li^+} &= S_1 - \frac{t_1}{x_1}\frac{q^*}{T} \end{aligned} \quad (28)$$

The two terms on the right hand side in Eq. (28) are unique for the two-component system. The entropy of a component in a mixture depends on the composition; for ideal mixtures $S_j = S_j^0 - R\ln x_j$. In a one-component system, $S^*_{CO_3^{2-}} + 2S^*_{M^+} = S_{M_2CO_3}$ [1].

The time to reach stationary state conditions can be estimated. Tyrrell [20] gives an expression for the time dependency of the Seebeck coefficient, valid for one degree of freedom for diffusion like here:

$$\frac{\alpha_{S,t} - \alpha_{S,0}}{\alpha_{S,\infty} - \alpha_{S,0}} = 1 - \frac{8}{\pi^2}\exp(-\frac{t}{\Theta}) \quad (29)$$

Here Θ is the 'characteristic time', which governs the rate at which the stationary state equilibrium is established for a constant ΔT. The characteristic time is defined by:

$$\Theta = \frac{h^2}{\pi^2 D_{12}} \quad (30)$$

Here π is the mathematical constant, h is the actual distance between the electrodes through the porous material and D_{12} is the interdiffusion coefficient. The tortuosity is here unknown, so we can only use Eq. (30) to give an order-of-magnitude estimate of Θ. With $h = 5$ cm (the distance used in the experiments) and $D_{12} = 10^{-7}$ m^{2}s^{-1} $\Theta = 14$ h. With $h = 10$ cm, $\Theta = 28$ h and it takes 5Θ to achieve 99.5 % of the stationary state value. A distance between the electrodes larger than 10 cm may be relevant in our system, meaning that the stationary state needs more than five days to establish itself. This means that Eq. 26 is relevant for interpretation of a measurements that lasts a few hours. It also means that an experiment must be carried out over more than a day, in order to be able to probe a Soret effect.

2.4. The Seebeck coefficient of cell LMC-MgO at stationary state

We add the contributions to the Seebeck coefficient from the five subsystems; Eq. (4), Eq. (8) and Eq. (25) and obtain the Seebeck coefficient for $J_{21} = 0$ (Soret equilibrium):

$$\alpha_{S,\infty} = -\frac{1}{F}\left[\frac{1}{2}S_{CO_2} + \frac{1}{4}S_{O_2} + S^*_e - \frac{1}{2}S^*_{CO_3^{2-}}\right] \quad (31)$$

This expression is exactly the same as the expression obtained for the one-component system [1]. We will use Eq. (31) to calculate the transported entropy of the carbonate ion from measured values of $(\alpha_S)_\infty$, using knowledge of the transported entropy of the electron and of the equation of state for the gases, see Section 4.3.

With the entropy relation for ideal gases ($dS_j = C_{p,j}dT/T - Rdp_j/p_j$), we express the temperature variation in the Seebeck coefficient as:

$$\left(\frac{d\alpha_S}{d\ln T/T^r}\right)_{p_{CO_2},p_{O_2}} = -\frac{1}{F}\left(\frac{1}{2}C_{p,CO_2} + \frac{1}{4}C_{p,O_2} + \tau_e - \frac{1}{2}\tau_{CO_3^{2-}}\right) \quad (32)$$

where T^r is any reference temperature (we take 298 K), $C_{p,j}$ and τ are, respectively, the heat capacity of component j and the Thomson coefficient of the charge carriers. The Thomson coefficient can in principle be positive or negative [21]. The variation in α_s with the partial pressures of carbon dioxide and of oxygen are (ideal gas):

$$\left(\frac{d\alpha_S}{d\ln p_{CO_2}/p^0}\right)_{T,p_{O_2}} = \frac{R}{2F} = 0.043\,\text{mV K}^{-1} \quad (33)$$

Table 2
Composition of the gas mixtures used in the experiments.

Gas mixture	CO_2(%)	O_2(%)	He(%)
1	66	34	0
2(AGA)	7.3	0.1	92.6
3	7.3	3.7	89
4	7.3	10	82.7
5	7.3	33	59.7
6(AGA)	7.3	80	12.7
7	20	33	47

$$\left(\frac{d\alpha_S}{d\ln p_{O_2}/p^0}\right)_{T,p_{CO_2}} = \frac{R}{4F} = 0.022\,\text{mV/K}^{-1} \quad (34)$$

Here p^0 is the standard pressure of 1 bar. The absolute value of α_s will increase with decreasing partial pressures.

3. Experimental

The experimental set-up was described in [1], see also Fig. 1b.

An initial study was first made to assess the state of the experiment. The time-stability of the Seebeck coefficient was investigated by recording the development of the Seebeck coefficient over 8 hours, and by recording one temperature difference and the corresponding potential over a period of 5 days. In the first of these experiments the electrodes were initially kept at the same temperature. The electrode positions were fixed at a distance of about 5 cm. An extra heating element, placed under the crucible, was used to produce a temperature difference between the electrodes. This heating element was made of resistance wire wrapped around the walls of an alumina tube. An alumina disk was placed on top of the element to avoid short-circuiting. The total resistance of the wire was 30 Ω. A k-type thermocouple was placed near the heating element to control the power supply. A temperature difference evolved when power was added to the extra heating element. When the emf and ΔT reached a stable value, the power supply to the heating element was again turned off. In the long-term experiment lasting 5 days, the electrode positions were fixed, and the temperature difference kept constant. The Seebeck coefficients were next measured at stationary state (Soret equilibrium) conditions. Gold and platinum were used as electrode materials, and molten carbonate mixtures with Na^+ or K^+ were studied in combination with Li^+. Table 1 gives the composition of the electrolytes used in the experiments and the mixture's melting point temperature. The gas composition were varied as shown in Table 2. Lithium carbonate (Li_2CO_3) with purity > 99 %, sodium carbonate (Na_2CO_3) with purity ≥ 99 %, potassium carbonate (K_2CO_3) with purity ≥ 99 % and magnesium oxide with purity > 99 % were obtained from Sigma Aldrich. All chemicals were used without further purification. Premade gas mixtures of carbon dioxide and oxygen were purchased from Yara Praxair unless other supplier (AGA) is specified.

Dispersions of the binary alkali carbonates (see Table 1) and MgO(s) were prepared according to the procedure described in [1]. After drying, the electrolyte was melted at a constant temperature in the vertical tube furnace and kept at this temperature for at least 48 hours to ensure stable conditions. All experiments were performed in a Nitrogen atmosphere. No deterioration of the alumina crucible or the alumina tubes were observed after the experiment.

The average temperature of the experiment was either 550, 650, 750 or 850 °C. The temperature difference was always smaller than 20 °C, to avoid the need of temperature corrections in the Seebeck coefficient. The gas mixture (in most cases with the composition 66 % CO_2 and 34 % O_2) was passed through the 5-bore ceramic tube for at least 5 hours before the experiment started. A slow flow rate, adapted for good gas-metal-electrolyte contact was used.

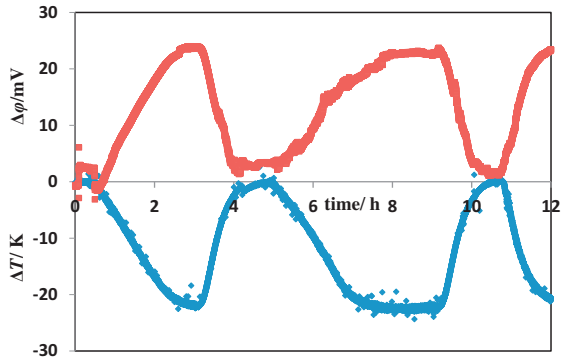

Fig. 3. The measured emf $\Delta\phi$ and temperature difference ΔT for cell LNC-MgO for the initial time conditions. The electrodes were gold and $p_{CO_2} = 0.66$ and $p_{O_2} = 0.34$ bar.

The presence of the solid magnesium oxide prevented convective mixing, but allowed in principle a concentration gradient to be formed in the temperature gradient (Soret effect).

In all experiments, the temperature and electric potential were measured every third second. The experiment started when the temperatures and the electric potential were stable. The measured potential, at a given temperature and for a given gas mixture, were plotted against the temperature difference. The Seebeck coefficients were the slopes of these plots, see *e.g.*, Fig. 5. For the cell LNC-MgO, one series of measurements was reproduced three times, by replacing the electrolyte completely between each experiment. The uncertainty, $\pm 0.02\,mV\,K^{-1}$, obtained by this reproduction of measurements, was larger than the double standard deviation from linear regression.

4. Results and Discussion

4.1. The time-evolution

We discuss first the time-dependency of the Seebeck coefficient for cell LMC-MgO, and conclude from the measurements that we can use the stationary state expression (Eq. (31)) to interpret the results. For experiments that we consider to be at initial times (up to 8 hours), the measured potential variation was all the time proportional to the temperature variation, see Fig. 3 for results from cell LNC-MgO.

The long-term experiment over 5 days, did not alter the potential within the accuracy of the experiments, see Fig. 4. Gas is slowly bubbling through the cell at the electrodes, but this will not prevent a Soret equilibrium to form in the electrolyte with dispersed oxide. (In the absence of the solid oxide in the binary carbonate

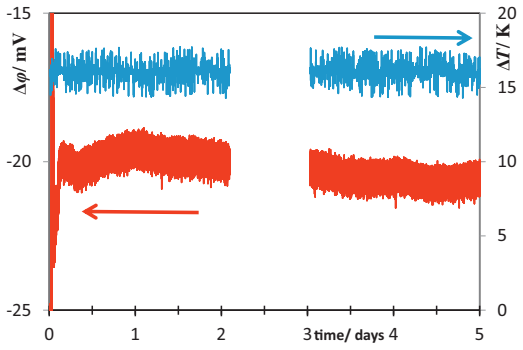

Fig. 4. The measured $\Delta\phi$ and temperature difference ΔT for cell LNC-MgO for the long-term experiments. The electrodes were platinum, the average temperature 550 °C and $p_{CO_2} = 0.66$ and $p_{O_2} = 0.34$ bar.

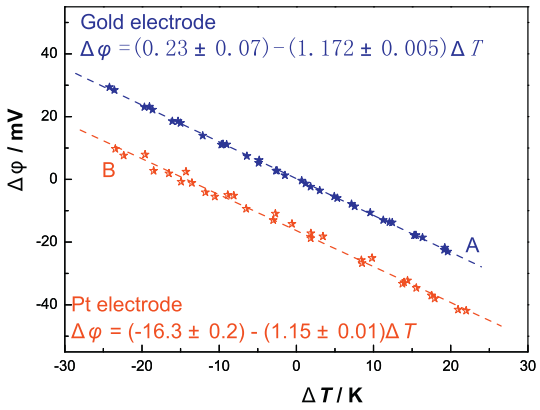

Fig. 5. The measured potential versus the temperature difference across the cell LNC-MgO(s) for Au(s) (A) and Pt(s) (B) electrodes. The average temperature was 550 °C and the electrode gas partial pressures $p_{CO_2} = 0.66$ $p_{O_2} = 0.34$. The equations are the linear regressions (dotted lines) and the accuracy is a double standard deviation from the regression analysis.

mixture, it was not possible to obtain a stable value.) The lack of an observed time-dependence of the Seebeck coefficient supports the possibility that the term involving q^* in the Seebeck coefficient is negligible, *c.f.* Eq. (26), and that Eq. (31) can be used to interpret the results. This shall be done in the following.

4.2. Stationary state

Seebeck coefficients for binary mixtures of alkali carbonate electrolytes are shown under various conditions in Figs. 5–7 and in Table 3. The values are all larger than those obtained with pure lithium carbonate and for dispersions of lithium carbonate with inorganic powders (−0.88 to $-1.05\,mV\,K^{-1}$ [1]). Before we discuss these encouraging results, we report on other tests on the cell's performance.

4.2.1. Effect of electrode material

To test the influence of the choice of electrode materials, gold was replaced by platinum. The mechanism of the electrode reaction can vary slightly between the metals, since oxide layers are more easily formed on platinum [23,24]. The results for the Seebeck coefficient, shown in Fig. 5, are the same within the accuracy of the experiment, compare -1.17 to $-1.15 \pm 0.02\,mV\,K^{-1}$. This fact means that the electrode reaction is most probably the same on both electrodes, and that the transported entropies of the electrons are close to each other. According to the literature, they are both small, around $0.4\,J\,K^{-1}\,mol^{-1}$ for Au at 730 °C [25] and around $2\,J\,K^{-1}\,mol^{-1}$ for Pt at 730 °C [26].

The two electrode materials differ in their bias potential, as can be seen from Fig. 5. A bias potential can arise due to small differences in the metal surface in two electrodes of the same kind. The difference is larger for two platinum electrodes (here 16 mV) than for two gold electrodes (here 0.23 mV). Even if most

Table 3
The Seebeck coefficient (α_S) and the transported entropy of the carbonate ion for all electrolytes. The electrodes were gold, the partial pressures $p_{CO_2} = 0.66$ and $p_{O_2} = 0.34$ bar and T is the average of the electrode temperatures. Data for the single carbonate system were reported in [1]. The uncertainty is a double standard deviation, estimated from measurements repeat.

Cell	T	α_S	$S^*_{CO_3^{2-}}$
	°C	$mV\,K^{-1}$	$J.K^{-1}\,mol^{-1}$
LC-MgO	750	-1.04 ± 0.02	201 ± 4
LKC-MgO	750	-1.13 ± 0.02	184 ± 4
LNC-MgO	750	-1.25 ± 0.02	161 ± 4

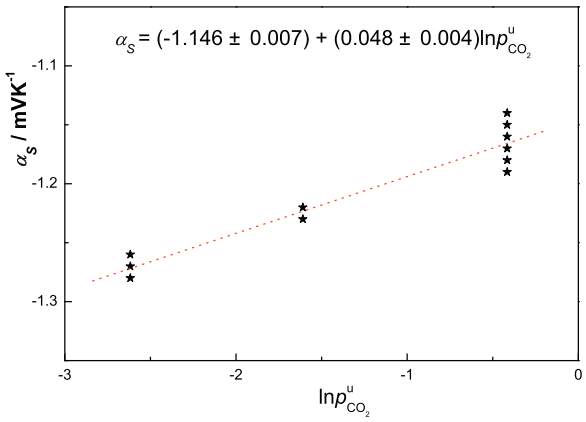

Fig. 6. The Seebeck coefficient as a function of the partial pressure of carbon dioxide p_{CO_2} for the cell LNC-MgO. The electrodes were Au(s), the average temperature were 550 °C and the $p_{O_2} = 0.33$ bar. The equation is the linear regression, shown by the dotted line, and the uncertainty is the double standard deviation from the regression analysis.

results for platinum gave a lower value than this, they were on the average larger than for gold. This confirms our expectation that the platinum surface is less inert in molten alkali carbonates [23,24]. The formation of an oxide layer may disturb the measurements and the correlation with the theory. We continued the investigations using the most inert material, gold.

4.2.2. Effect of pressure - and temperature variations

In view of the discussion above on possible side reactions, we investigated the pressure and temperature variations of the Seebeck coefficient of the cell LNC-MgO. The pressure variation is shown in Figs. 6 and 7.

As shown in Section 2.4, Eqs. (33) and (34), the slope of the Seebeck coefficient versus $\ln p_j/p^0$ is fixed, for a given electrode reaction. The electrode reaction (Eq. (1)) gives the theoretical slopes 0.043 and 0.021 mV K^{-1} for a varying partial pressure of carbon dioxide or oxygen gas, respectively. The experimentally determined values of 0.048 ± 0.004 mV K^{-1} and 0.0134±0.005 (see Figs. 6 and 7) confirm the electrode reaction within the uncertainties of the experiment. This enables us to use Eq. (31) to predict the Seebeck coefficient with respect to variations in the partial pressures of carbon dioxide and oxygen (see below). Lower gas partial pressures

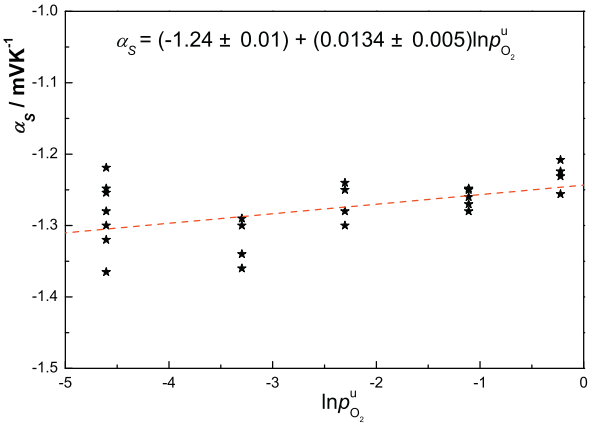

Fig. 7. The Seebeck coefficient as a function of the partial pressure of oxygen p_{O_2} for the cell LNC-MgO. The electrodes were Au(s), the average temperature was 550 °C and the $p_{CO_2} = 0.073$ bar. The equation is the linear regression, shown by the dotted line, and the uncertainty is the double standard deviation from the regression analysis.

gives an increase in the absolute value of the Seebeck coefficient (makes it more negative).

The temperature variation of the Seebeck coefficient, as determined from a plot of the Seebeck coefficient versus the logarithm of the temperature, see Eq. (32), gave a negative slope of −0.60 ±0.07 mV K^{-1}. When we raise the cell average temperature from 550 to 850 °C, we increase the absolute value of the Seebeck coefficient by 0.2 mV K^{-1}.

4.3. The transported entropy of the carbonate ion

Table 3 shows the data collected for the Seebeck coefficient and the calculated transported entropy of the carbonate ion for all cells investigated. For the sake of comparison with cell LC-MgO, reported previously [1], we show the results for the cell average temperature 750 °C. We calculated the transported entropy of the carbonate ion from Eq. (31). Standard entropies of the gases were 271 and 244 J K^{-1} mol^{-1} (750 °C, HSC Chemistry) for CO_2 and O_2, respectively, and the transported entropy of the electron in the gold conductor was 0.4 J K^{-1} mol^{-1} [25].

The Seebeck coefficient increases significantly in absolute value by adding sodium or potassium to the lithium carbonate. This is due to a reduction in the transported entropy of the carbonate ion, see values given in Table 3. Jacobsen and Broers [12] reported Seebeck coefficients of −1.14 to −1.20 mV K^{-1} for dispersions of binary and ternary equimolar mixtures of alkali carbonates with magnesium oxide. Their values compare well to our results. However, they concluded, from variations in their measured values, that the Seebeck coefficient was independent of the melt composition investigated, while we find that there is a dependency (see Table 3). Here, the cell LNC-MgO gave the largest Seebeck coefficient. The cell LKC-MgO was here not an equimolar mixture, which may explain the deviation from the results of Jacobsen and Broers. Also their experimental procedure differed from this study: they collected only one set of temperature data and potential data at each temperature and decomposed the data with a multiple regression analysis. We determined the Seebeck coefficient from plots of the emf $\Delta\phi$ versus the temperature difference, at constant average cell temperature. They reported values for the temperature range (530-880 °C), while we report for a given average temperature and find that there is a temperature variation. More experiments, together with a fundamental theoretical understanding of the transported entropy, are required to elucidate on the effect of melt composition.

Our previous study [1] showed that adding a solid inorganic phase to the pure lithium carbonate significantly reduced the value of $S^*_{CO_3^{2-}}$. We concluded that this was due to a reduction in the entropy of the lithium carbonate ($S_{Li_2CO_3}$), caused by the presence of the solid particles in the dispersion. In this study, we see that introduction of larger cations to the system further decreases the value of $S^*_{CO_3^{2-}}$. Below, we discuss two factors that can affect the value of the transported entropy.

For the binary mixtures, the molar entropy of the component in the mixture and the heat of transfer limit the values of the transported entropies (see the relations given in Eq. 28). The molar entropy of a component is generally larger in a mixture compared to the pure component value. Using the ideal mixture approximation, $S_j = S^0_j - R\ln x_j$ with $S_{Li_2CO_3} = 309$ J K^{-1} mol^{-1} and mole fractions given in Table 1, we estimated the entropy of lithium carbonate in the two binary mixtures to raise 4 or 5 J K^{-1} mol^{-1} above the pure-component value. This trend is opposite to that of the transported entropy of carbonate ion. Above, we concluded that the term containing the heat of transfer in Eq. (26), $\left(\frac{t_2}{x_2} - \frac{t_1}{x_1}\right)\frac{q^*}{T}$, is small. This could well be because difference in the transference coefficient of the two salts is small, $\left(\frac{t_2}{x_2} - \frac{t_1}{x_1}\right)$, not necessarily q^*.

If so, the term involving the heat of transfer in Eq. (28) could be responsible for the lowering of the sum of the transported entropies of the two ions (the left-hand side of the relations in Eq. (28)). Then, the heat of transfer is positive and cause the transported entropy of the carbonate ion to be lower in the binary mixture than in the pure lithium carbonate. The relations in Eq. (28) limit the values of the transported entropies of the ions in the mixture, but what determines the distribution between the cations and the anions? The local structure in the melt may affect the answer, with enthalpic as well as entropic effects. Introduction of larger cations affects the melt structure. Studies have shown [27,28] that the addition of sodium or potassium to the pure lithium carbonate introduces changes in the short-range structure of the melt. Tissen et. al [27] found from molecular dynamics simulations, that introduction of sodium or potassium in the lithium carbonate increased the distance between carbonate ions in the melt [27]. Moreover, the association Li^+-CO_3^{2-} was tightened while the association M^+-CO_3^{2-} was loosened compared to the pure carbonates. Clearly, more theoretical and experimental efforts, are both needed to understand the nature of the transported entropy.

4.4. Practical perspectives

We have seen above that cells with alkali carbonates and gas electrodes gives Seebeck coefficients in the order of $-1\ mV\ K^{-1}$. Furthermore, we have found that the value of the coefficient depends on melt composition, temperature and composition of the electrode gas. The addition of either sodium or potassium carbonate, together with an inorganic powder, to the molten lithium carbonate enhances the Seebeck coefficient. To generate a large potential, a large temperature difference between the electrodes are required. By using mixtures as electrolytes, we open up for this possibility, as they have lower melting points compared to the pure components and thus allows a larger range of operating temperatures. A temperature difference of 200 degrees across a single cell, will therefore represent 0.2 V.

The cell LMC-MgO can not only utilize waste heat, but also off-gases containing carbon dioxide and oxygen. We have found that a lowering of the gas partial pressures of carbon dioxide and oxygen, increases the Seebeck coefficient. The off-gas from a silicon furnace contains CO_2, O_2, N_2, H_2O and various other components. By using the off-gas, containing 1.5 % CO_2 and 20 % O_2, as electrode gas on the two sides, we estimate from Eq. (31) with the ideal gas relation and data in Table 3, that the Seebeck coefficient for cell LNC-MgO at 750 °C rises to $-1.4\ mV\ K^{-1}$. The contribution to the single cell thermoelectric potential becomes 0.30 V for a ΔT of 200.

The off-gas from the silicon furnace, at a different composition than air, has an additional potential for power production. Consider using a concentration cell in series with the thermoelectric cell LMC-MgO at the lower temperature of the cell. The additional potential can be calculated from the expression for a concentration cell

$$\Delta\phi_{conc} = -\frac{RT}{F}\ln\frac{p_{CO_2,a}^{1/2}p_{O_2,a}^{1/4}}{p_{CO_2,c}^{1/2}p_{O_2,c}^{1/4}} \tag{35}$$

To use furnace off-gas as anode gas (a) and air as cathode gas (c) at 550 °C, enhances the cell potential by 0.14 V using the same materials and utilizing the chemical exergy of the off-gas. For the thermoelectric and the concentration cell in series, this gives an order of magnitude of 0.5 V when $\Delta T = 200$ K. We propose therefore a system for thermoelectric energy conversion that also can benefit from off-gases containing CO_2.

Much work remains before such an idea can be realized. The potential for work delivery is only one of many considerations. The internal power losses and materials properties and costs are also essential [29]. A first evaluation of the performance of a thermoelectric cell is often done by calculating the figure of merit, where the electrical, σ, and thermal, λ, conductivity at zero current also enters [30], see however [6] for electrochemical cells. The dimensionless figure of merit is:

$$ZT = \frac{\alpha_S^2\sigma}{\lambda}T \tag{36}$$

A high ZT means that a high conversion from thermal to electric energy is likely. In order to estimate ZT, we used the electrolyte values for the thermal and electric conductivity, since we believe that the electrolyte values dominate the values for the whole device. The cell LC has $\lambda_{LC} = 1\ W\ m^{-1}\ K^{-1}$ [31] while cells LC-MgO and LNC-MgO has $\lambda_{effective} = 0.60\lambda_{LC} + 0.40\lambda_{MgO}$, where λ_{MgO} was $18\ W\ m^{-1}\ K^{-1}$ (at 400 °C) [32], and 0.60 and 0.40 was the volume fraction of the liquid and the MgO, respectively. The electrical conductivities of the dispersions were set as 80 % of the values of the alkali carbonates (this was estimated from [13]). Values for ZT is shown in Table 4.

Table 4
Measured Seebeck coefficients for three cells, electrical and thermal conductivities for the alkali carbonates are from [36,37].

cell	T °C	α_S mV K^{-1}	σ ohm^{-1} cm^{-1}	λ W m^{-1} K^{-1}	ZT
LC	750	-0.88 ± 0.06	4.24	1	0.34
LC-MgO	750	-1.04 ± 0.02	3.4*	7.8	0.05
LNC-MgO	750	-1.25 ± 0.02	2.2*	7.8	0.05

* 80 % of the value for the molten alkali carbonate with no added solid

Without having done any optimisation, it is encouraging to observe that the LC cell obtains a value of 0.34. This can be compared with various solid state thermoelectric materials [33]. For materials suitable for a hot side temperature of 800 °C, they reported that a lead telluride compound gave $ZT = 1.45$ at 425 °C. Culp reported $ZT = 0.8$ at 800 °C for n-type Sb-doped MNiSn (M= Ti, Zr, Hf) [34]. The addition of the inorganic powder significantly increases the Seebeck coefficient. At the same time it seems to reduce the ZT. More knowledge is needed on how the Seebeck coefficient varies with the amount and type of solid phase, and also how the inorganic phase affects the electrical and thermal conductivity. The composition of the alkali carbonate mixture dictates the operating temperature range and determines the melt conductivity [35], and it would be interesting to also study further the Seebeck coefficient as a function of composition.

We finally estimate the power density P/A of the thermoelectric device in combination with the concentration cell at matched load conditions from [7]:

$$P/A = \frac{1}{4}\frac{(\alpha_s\Delta T + \Delta\phi_{conc})^2}{rl} \tag{37}$$

Using cell LNC-MgO as example, we use the Seebeck coefficient and electrical resistivity ($r = \sigma^{-1}$) as given in Table 4. Again we assume that the electrolyte gives the largest contribution to the resistance. With an electrolyte thickness (l) of 5 mm, and $\Delta T = 100$ K, we obtain a power density of $0.8\ kW\ m^{-2}$. Assuming that losses during operation can halve this value, one should expect a power density with an order of magnitude of $0.5\ kW\ m^{-2}$.

5. Conclusions

We have reported theoretical and experimental results for a system which can be interesting for thermoelectric energy conversion. The system is described with non-equilibrium thermodynamics. Seebeck coefficients up to -1.4 mV K^{-1} can be realized with molten carbonate mixtures as electrolytes and electrode gas composition like that of the off-gases from the silicon furnace. A single thermoelectric converter, operating with a difference of 200 K, yields

0.30 V. By adding a concentration cell operating on off-gases and air, an additional 0.14 V can be added to the cell emf. This idea might be relevant for commercial exploitation as a wide range of industrial processes have off-gases of composition different from air, containing carbon dioxide and oxygen. A figure of merit near 0.3 and a power density near 0.5 kW m^{-2} seem within reach already. Much work remains to be done to optimize these factors.

Acknowledgment

The authors are grateful for the project "Next generation thermoelectric energy converters", project no. 221672 from the Research Council of Norway. M.T.B. acknowledges the Research Council of Norway (project no. 193161) and the Norwegian Ferroalloy Producers Research Association for funding through the project "Fugitive emissions of materials and energy".

ENERSENSE is acknowledged for financial support.

References

[1] M.T. Borset, X. Kang, O.S. Burheim, G.M. Haarberg, Q. Xu, S. Kjelstrup, Seebeck coefficients of cells with lithium carbonate and gas electrodes, Electrochimica Acta (2015), xx:y-xy.
[2] J.N. Agar, in: P. Delahay (Ed.), Advances in Electrochemistry and Electrochemical Engineering, Interscience, New York, 1963, chapter Thermogalvanic cells.
[3] G.Jeffrey Snyder, Eric S. Toberer, Complex thermoelectric materials, Nature materials 7 (2) (2008) 105–114.
[4] L.E. Bell, Cooling, heating, generating power, and recovering waste heat with thermoelectric systems, Science 321 (2008) 1457–1461.
[5] Gunawan Andrey, Chao-Han Lin, Daniel A. Buttry, Vladimiro Mujica, Robert A. Taylor, Ravi S. Prasher, Patrick E. Phelan, Liquid thermoelectrics: review of recent and limited new data of thermogalvanic cell experiments, Nanoscale and Microscale Thermophysical Engineering 17 (4) (2013) 304–323.
[6] Theodore J. Abraham, Douglas R. MacFarlane, Ray H. Baughman, Liyu Jin, Na Li, Jennifer M. Pringle, Towards ionic liquid-based thermoelectrochemical cells for the harvesting of thermal energy, Electrochimica Acta 113 (2013) 87–93.
[7] Marit Takla, Odne S. Burheim, Leiv Kolbeinsen, Signe Kjelstrup, A solid state thermoelectric power generator prototype designed to recover radiant waste heat, in: Maria D. Salazar-Villalpando, Neale R. Neelameggham, Donna Post Guillen, Soobhankar Pati, Gregory K. Krumdick (Eds.), Energy Technology 2012: Carbon Dioxide Management and Other Technologies, March 2012.
[8] Schei Anders, Johan Kr. Tuset, Halvard Tveit, Production of High Silicon Alloys. Tapir, Trondheim, Norway, 1998.
[9] Nils Eivind Kamfjord *Mass and Energy Balances of the Silicon Process*. PhD thesis, NTNU, Trondheim, 2012.
[10] M. Takla, N. Kamfjord, H. Tveit, S. Kjelstrup, Energy and exergy analysis of the silicon production process, Energy 58 (2013) 138–146.
[11] H.V.M. Hamelers, O. Schaetzle, J.M. Paz-Garca, P.M. Biesheuvel, C.J.N. Buisman, Harvesting energy from co2 emissions, Environmental Science & Technology Letters 1 (1) (2014) 31–35.
[12] T. Jacobsen, G.H.J. Broers, Single Electrode Heat Effects I. Peltier Heats of Gas Electrodes in Carbonate Paste Electrolytes, J. Electrochem. Soc. 124 (1977) 207–210.
[13] Mizuhata Minoru, Yasuyuki Harada, Guem ju Cha, Alexis Bienvenu Béléké, Shigehito Deki, Physicochemical Properties of Molten Alkali Metal Carbonates Coexisting with Inorganic Powder, J. Electrochem. Soc. 5 (2004) E179–E185.
[14] José A Manzanares, Miikka Jokinen, Javier Cervera, On the different formalisms for the transport equations of thermoelectricity: A review, Journal of Non-Equilibrium Thermodynamics (2015).
[15] S.R. de Groot, P. Mazur, Non-Equilibrium Thermodynamics, Dover, London, 1984.
[16] K.S. Førland, T. Førland, S. Kjelstrup, Irreversible Thermodynamics. Theory and Application, 3rd edition, Tapir, Trondheim, Norway, 2001.
[17] S. Kjelstrup, D. Bedeaux, Non-equilibrium thermodynamics of heterogeneous systems, World Scientific, Singapore, 2008.
[18] van P.F. Velden, Equilibrium between (Li,Na,K,Mg)-Carbonate Melt, Gaseous CO_2 and MgO, Trans Faraday Soc. 63 (1967) 175–184.
[19] S. Kjelstrup Ratkje, H. Rajabu, T. Førland, Transference coefficients and transference numbers in molten salt mixtures relevant for the aluminium electrolysis, Electrochim. Acta 38 (1993) 415–423.
[20] H.J.V. Tyrrell, Diffusion and Heat Flow in Liquids, Butterworths, London, 1961.
[21] J. J Lander, Measurements of Thomson Coefficients for Metals at High Temperatures and of Peltier Coefficients for Solid-Liquid Interfaces of Metals, Physical Review 74 (1948) 479–488.
[22] G.J. Janz, Molten carbonate electrolytes as acid-base solvent systems, Journal of Chemical Education 44 (1967) 581–590.
[23] G.J. Janz, F. Saegusa, The oxygen electrode in fused electrolytes, Electrochimica Acta 7 (1962) 393–398.
[24] G.J. Janz, A. Conte, Potentiostatic Polarization Studies In Fused Carbonates I. The Noble Metals, silver and nickel, Electrochimica Acta 9 (1964) 1269–1278.
[25] C.Y. Ho, R.H. Bogaard, T.C. Chi, T.N. Havill, H.M. James, Thermoelectric power of selected metals and binary alloy systems, Thermochimica Acta 218 (1993) 29–56.
[26] J.P. Moore, R.S. Graves, Absolute Seebeck coefficients of platinum from 80 to 340 K and the thermal and electrical conductivities of lead from 80 to 400 K, Journal of Applied Physics 44 (1973), 1174-.
[27] J.T.W.M. Tissen, G.J.M. Janssen, J.P. van der Eerden, Molecular dynamics simulation of binary mixtures of molten alkali carbonates, Molecular Physics 82 (1994) 101–111.
[28] S. Kohara, Y.S. Badyal, N. Koura, Y. Idemoto, S. Takahashi, L.A. Curtiss, M.L. Saboungi, The structure of molten alkali carbonates studied by neutron diffraction and *ab initio* calculations, J. Phys. Condens. Matter 10 (1998) 3301–3308.
[29] Shannon K. Yee, Saniya LeBlanc, Kenneth E. Goodson, Chris Dames, $ per W metrics for thermoelectric power generation: beyond ZT, Energy Environ. Sci. 6 (9) (2013) 2561–2571.
[30] Howard Littman, Burton Davidson, Theoretical bound on the thermoelectric figure of merit from irreversible thermodynamics, Journal of Applied Physics 32 (2) (1961) 217–219.
[31] X. Zhang, H. Wicaksono, S. Fujiwara, M. Fujii, Accurate measurements of thermal conductivity and thermal diffusivity of molten carbonates, High Temperature-High pressures 34 (2002) 617–625.
[32] W.M. Haynes, D.R. Lide, T.J. Bruno, CRC Handbook of Chemistry and Physics, 95th electronic edition, CRC Press, 2014.
[33] Saniya LeBlanc, Shannon K. Yee, Matthew L. Scullin, Chris Dames, Kenneth E. Goodson, Material and manufacturing cost considerations for thermoelectrics, Renewable and Sustainable Energy Reviews 32 (2014) 313–327.
[34] Slade R. Culp, S.Joseph Poon, Nicoleta Hickman, Terry M. Tritt, J. Blumm, Effect of substitutions on the thermoelectric figure of merit of half-Heusler phases at 800 C, Applied Physics Letters 88 (4) (2006) 042106.
[35] V. Lair, V. Albin, A. Ringuedé, M. Cassir, Theoretical predictions vs. experimental measurements of the electrical conductivity of molten Li_2CO_3-K_2CO_3 modified by additives, international journal of hydrogen energy 37 (24) (2012) 19357–19364.
[36] G.J. Janz, M.R. Lorenz, Molten carbonate electrolytes: Physical properties, structure and mechanism of electrical conductance, Journal of the Electrochemical Society 108 (1962) 1052–1058.
[37] A.T. Ward, G.J. Janz, Molten carbonate electrolytes: electrical conductance, density and surface tension of binary and ternary mixtures, Electrochimica Acta 10 (1965) 849–857.